MOL PHARM

Inhibition of Neuronal Calcium Channels by a Novel Peptide Spider Toxin, DW13.3

KATHY G. SUTTON, CHET SIOK, ANTHONY STEA, GERALD W. ZAMPONI, STEVEN D. HECK, ROBERT A. VOLKMANN, MICHAEL K. AHLIJANIAN, and TERRY P. SNUTCH

Biotechnology Laboratory, University of British Columbia, Vancouver, B.C., Canada V6T 1Z3 (K.G.S., A.S., G.W.Z., T.P.S.), and Departments of Neuroscience (C.S., M.K.A.) and Medicinal Chemistry (R.A.V.), Pfizer, Inc., Groton, Connecticut

This paper is available online at http://www.molpharm.org

ABSTRACT

Peptide toxins have proved to be useful agents, both in discriminating between different components of native calcium channel currents and in the molecular isolation and designation of their cloned channel counterparts. Here, we describe the isolation and characterization of the biochemical and physiological properties of a novel 74-amino acid peptide toxin (DW13.3) extracted from the venom of the spider *Filistata hibernalis*. The subtype specificity of DW13.3 was investigated using calcium channel currents recorded from two separate expression systems and several different cultured mammalian cell preparations. Overall, DW13.3 potently blocked all native calcium channel currents studied, with the exception of T-type currents recorded from GH3 cells. Examination of transiently expressed calcium channels in oocytes showed that DW13.3 had the highest affinity for α1A, followed by α1B > α1C > α1E. The affinity of DW13.3 for α1B N-type currents varied by 10-fold between expressed channels and native currents. Although block occurred in a similar 1:1 manner for all subtypes, DW13.3 produced a partial block of both α1A currents and P-type currents in cerebellar Purkinje cells. Selective occlusion of the P/Q-type channel ligand ω-conotoxin MVIIC (but not ω-agatoxin IVA) from its binding site in Purkinje neurons suggests that DW13.3 binds to a site close to the pore of the channel. The inhibition of different subtypes of calcium channels by DW13.3 reflects a common "macro" binding site present on all calcium channels except T-type.

High affinity block of calcium channels by a number of polypeptide toxins has aided in the pharmacological dissection of endogenous whole-cell currents present in different neuronal preparations. Toxins also have played an important role in the molecular isolation and characterization of different calcium channel subtypes in expression systems (for review see Olivera *et al.,* 1994). Neuronal calcium channels are multiprotein complexes composed of at least three subunits (α1, α2δ, and β), of which the distinct pore-forming α1 subunit (modulated by α2δ and β subunits) determines the major biophysical and pharmacological properties of the channel (Stea *et al.*, 1995b). Most neurons coexpress multiple types of different calcium channel α1 subunits (α1A–α1E, α1G; Snutch *et al.,* 1990; Soong *et al.,* 1993; Perez-Reyes *et al.*, 1998). Biophysical and pharmacological criteria have been used to isolate individual components of native whole-cell calcium currents (T-, L-, N-, and P/Q-type see Bean, 1989; Zhang *et al.*, 1993) and to identify their cloned counterparts; P/Q-type (α1A), N-type (α1B), L-type (α1C and α1D), and T-type (α1G) (Stea *et al.*, 1995b; Perez-Reyes *et al.*, 1998). Irreversible inhibition by ω-CgTX GVIA, a peptide fraction isolated from the venom of the fish-hunting cone snail *Conus geographus* (Olivera *et al.*, 1984), has been widely adopted as a defining characteristic of the α1B (N-type) calcium channel (Fox *et al.*, 1987; Dubel *et al.*, 1992; Boland *et al.*, 1994). ω-Aga IVA, a peptide toxin isolated from the venom of the spider *Agelenopsis aperta* (Mintz *et al.*, 1992a, 1992b), and another peptide fraction from the cone shell *Conus magus*, ω-CTx MVIIC (Hillyard *et al.*, 1992), have been used to identify and investigate the role of α1A (P/Q-type) currents in a number of different neuronal preparations and expression systems (Mori *et al.*, 1991; Turner *et al.*, 1992; Takahashi and Momiyama, 1993; Stea *et al.*, 1994; Randall and Tsien, 1995).

Although peptide toxins have proved to be useful in distinguishing different calcium channel subtypes, the specificity of a number of these compounds is not absolute. For example,

ABBREVIATIONS: ω-CgTX, ω-conotoxin; ω-Aga, agatoxin; HEK, human embryonic kidney; ES-MS, electrospray-mass spectrometry; HPLC, high performance liquid chromatography; EGTA, ethylene glycol bis(β-aminoethyl ether)-*N,N,N′,N′*-tetraacetic acid; HEPES, 4-(2-hydroxyethyl)-1-piperazineethanesulfonic acid; DMEM, Dulbecco's modified eagle medium; MEM, minimum essential medium; FCS, fetal calf serum; BAPTA, 1,2-bis(2-aminophenoxy)ethane-*N,N,N′,N′*-tetraacetic acid.

ω-CTx MVIIC inhibits both high threshold Q- and N-type currents (Hillyard *et al.*, 1992; Schwartz *et al.*, 1993). In addition, two other peptide fractions isolated from the venom of *A. aperta* have been shown to block a variety of different mammalian calcium channels; ω-Aga IA inhibits T-, L-, and N-type currents in rat dorsal root ganglion neurons (Scott *et al.*, 1990), and ω-Aga IIIA produces a high affinity inhibition of N-, L-, and P-type channels in neurons as well as in cardiac L-type channels (Mintz *et al.*, 1991; Mintz, 1994).

In the current study, we focused on identifying and characterizing the subtype specificity of a novel peptide toxin fraction, designated DW13.3, isolated from the venom of the spider *Filistata hibernalis* (DW). We described the extraction and complete amino acid sequence of DW13.3 (molecular weight, 8668; 74 amino acids, 12 cysteines) and investigated DW13.3 block of four different neuronal calcium channels expressed in *Xenopus laevis* oocytes (α1A, α1B, α1C, and α1E). The inhibitory action of DW13.3 in oocytes was also compared and contrasted to that observed in a human embryonic kidney cell line stably expressing α1B together with α2δ and β1b (α1B HEK cells) and on a number of cultured mammalian neuronal preparations. DW13.3 produced a high affinity block of all the calcium channel currents investigated in this study (with the exception of low threshold T-type currents recorded in GH3 cells). The kinetics of toxin block and the relative efficacy of the toxin varied among preparations. In addition, DW13.3 produced a partial block of the α1A current expressed in oocytes and P-type current recorded in cultured rat Purkinje neurons.

Materials and Methods

Preparation, purification, and sequence analysis of DW13.3. Venom was obtained by electrical stimulation of the cephalothorax of live CO_2-anesthetized spiders (Bascur *et al.*, 1980), and pooled venom stored at $-80°$. Mass spectral information was obtained using ES-MS on a Finnigan TSQ-700 mass spectrometer fitted with an Analytica of Branford (Branford, CT) ES ionization source. Samples were dissolved in 0.1% trifluoroacetic acid to a concentration of $\sim$10 μM. The flow rate of this solution into the mass spectrometer was 1 μl/min with a sheath of liquid of 2-methoxyethanol. The instrument was scanned over the range of m/z 600-2200 or 400-1800 in the profile mode, and the resulting data were deconvoluted using Finnigan Biotech software. The resolution of the instrument was set such that average mass data (as opposed to monoisotopic data) were collected. For higher molecular mass samples (>4000 Da), accuracy was within 0.01%, whereas at lower masses, the accuracy was $\sim$0.4 Da. The averaging of multiple molecular ions of different charge states accounts for the improved accuracy at higher mass. Peptide sequencing was performed on a Hewlett-Packard G1005A sequencing system consisting of a G1000A sequencer, an on-line 1090 HPLC unit, and an associated computer system and software. Amino acid analysis was performed with an Applied Biosystems Model 420H hydrolyzer/derivatizer and a model 130 analyzer. Data were acquired and processed using the PE Nelson data system.

Transient expression of calcium channel cDNAs in *X. laevis* oocytes. Stage V and VI *X. laevis* oocytes were prepared and nuclear injections with cDNAs were performed as described previously (Stea *et al.*, 1995a). Direct intranuclear injections were undertaken with 10 nl of a mixture of rat brain cDNAs encoding calcium channel α1, α2δ, and β subunits in a 1:1:1 molar mix. The cDNA constructs have been described previously (Bourinet *et al.*, 1996, and references thererin). Two-microelectrode voltage-clamp experiments were performed after 3–6-day incubations with a GeneClamp 500 amplifier

(Axon Instruments, Burlingame, CA). Macroscopic currents were recorded as described (Stea *et al.*, 1995a) in a solution containing 4 mM $BaCl_2$, 38 mM KCl, 36 mM TEA-Cl, 5 mM 4-aminopyridine, 0.4 mM niflumic acid, 0.02 mM 5-nitro-2-(3-phenylpropylamine)benzoic acid, 5 mM HEPES, and 500 μg/ml cytochrome *c* (Sigma Chemical, St. Louis, MO), pH 7.6. The endogenous oocyte calcium-activated Cl^- current was completely suppressed by the injection of 10–30 nl of a solution containing 100 mM BAPTA-free acid (10 mM HEPES, pH titrated to 7.2 with CsOH) to chelate intracellular calcium (Charnet *et al.*, 1994). Samples of DW13.3 were resuspended as stock solutions (115 μM) in double-distilled water and stored at $-20°$ between experiments. The toxin was dissolved in the recording saline before application and perfused into the bath. An effective exchange of the chamber solution was achieved within 1–2 sec as judged by superperfusion of a solution containing 100 mM Cd^+ and monitoring the development of block. Unless otherwise stated, currents were elicited by a 0.067-Hz train of 400-msec pulses from a holding potential of -100 mV. Acquisition and data analysis were performed using pCLAMP (ver. 6.03) software (Axon Instruments). Data were filtered at 500 Hz, and in most cases, leak subtraction was carried out on-line using a P/4 protocol.

HEK and GH3 cells. Whole-cell patch-clamp recordings were carried out on a HEK 293 cell line stably expressing α1B, α2δ, and β1b (Zamponi *et al.*, 1997). Cells were split and plated at $\sim$10% confluency on glass coverslips in DMEM supplemented with 10% fetal bovine serum and 0.4 mg/ml neomycin. GH3 cells were purchased from American Tissue Culture Collection (Rockville, MD), plated at $\sim$30% confluency on glass coverslips, and incubated at 37° in Ham's F-10 medium supplemented with 15% horse serum and 2.5% fetal bovine serum for up to 1 week. Whole-cell patch-clamp recordings were performed using an Axopatch 200-A amplifier (Axon Instruments) linked to a personal computer equipped with pCLAMP v 6.0. Patch pipettes (Sutter borosilicate glass) showed typical resistances of 1.7–3.5 MΩ. The internal pipette solution contained 105 mM CsCl, 25 mM TEA-Cl, 1 mM $CaCl_2$, 11 mM EGTA, and 10 mM HEPES, pH 7.2. The external recording solution contained 5 mM $BaCl_2$, 1 mM $MgCl_2$, 10 mM HEPES, 40 mM TEA-Cl, 10 mM glucose, and 87.5 mM CsCl, pH 7.2. DW13.3 was perfused directly into the vicinity of the cells by means of a solenoid-driven microperfusion system. Currents typically were elicited from a holding potential of -100 mV to various test potentials using Clampex (Axon Instruments). Data were filtered at 1 kHz and recorded directly onto the hard drive of a computer.

Isolation of sympathetic neurons, Purkinje cells, and cerebellar granule cells. Sympathetic neurons were isolated from the superior cervical ganglia of 28–35-day-old male Sprague Dawley rats as described in by Shapiro and Hille (1993) with the exception that after 20 min in papain, the tissue was placed in 3 ml of Hanks' solution containing 3 mg/ml type I collagenase (Worthington Biochemicals, Freehold, NJ) and 10 mg/ml dispase type II (Boehringer-Mannheim, Indianapolis, IN). Purkinje cells from the cerebellar vermis were isolated according to the method of Regan (1991) with the following modifications. Tissue was incubated in 5.5 units/ml papain (Worthington) for 30 min at 32° and then transferred to room-temperature MEM containing 10% FCS and 10 mM glucose. The tissue was cut into $\sim$2-mm pieces and stored in the MEM solution under an atmosphere of 95% O_2/5% CO_2 at room temperature until needed. Cells were isolated for recording by gentle trituration in MEM containing 1 mg/ml DNase. Cerebellar granule cells were prepared by isolating the cerebellum from 8-day-old pups and mincing the tissue into $\sim$1-mm pieces in room-temperature Tyrode's solution. The tissue was washed in calcium/magnesium-free Tyrode's solution and incubated in 0.1% trypsin at 37° for 15 min. After incubation, the tissue was washed in Tyrode's solution with 10% FCS and triturated in the presence of DNase, spun, and plated onto poly-*d*-lysine-coated glass coverslips. The cells were maintained in an atmosphere of 5% CO_2 at 37° in MEM with Earle's salts supplemented with 10% FCS, 2 mM L-glutamine, 25 mM KCl, and 100

units/ml penicillin-streptomycin. Cultures were treated with 10 μM cytosine-arabinofuranoside 24 hr after plating to inhibit non-neuronal cells. Recordings were made 5–6 days after isolation.

Electrophysiology of native calcium currents. Currents were recorded at room temperature in the sympathetic, Purkinje, and cerebellar granule cells using whole-cell patch-clamp with an Axopatch 1D amplifier and pCLAMP software (Axon Instruments). The electrodes had tip diameters of 1–2 μm with a resistance of 1.5–2.5 MΩ. Corrections were made for junction potentials, and leak currents were subtracted using a standard P/N protocol provided by the software. Seals were formed in a standard extracellular buffer containing 150 mM NaCl, 4 mM KCl, 10 mM HEPES, 10 mM D-glucose, 2 mM MgCl$_2$, and 2 mM CaCl$_2$, pH 7.4, and adjusted to 335 mOsM using sucrose. Barium currents were recorded using a buffer containing 154 mM TEA-Cl, 10 mM HEPES, 10 mM D-glucose, and 2 mM MgCl$_2$, pH 7.4, adjusted to 335 mOsm with sucrose and containing either 5 mM BaCl$_2$ for sympathetic and Purkinje cells or 10 mM BaCl$_2$ for granule cells. The intracellular buffer contained 108 mM CsCl, 9 mM HEPES, 9 mM EGTA, 4 mM MgCl$_2$·6H$_2$O, 14 mM creatine-PO$_4$, 4 mM MgATP, and 0.3 mM Tris-GTP, pH 7.4, and adjusted to 320 mOsM with sucrose.

Data analysis. Current recordings were analyzed using pCLAMP software (Axon Instruments), and curve fitting was carried out with GraphPAD Prism Software (San Diego, CA). Preparation of figures was carried out in Freelance graphics (Windows). Unless otherwise stated, error bars represent the standard error.

Results

Isolation and sequence analysis of DW13.3. An ion exchange chromatogram of crude *F. hibernalis* (DW) venom is shown in Fig. 1. A protocol using both ion exchange and reverse-phase HPLC separated DW13.3 from the other *Filistata* (DW) peptides. Accordingly, crude *F. hibernalis* (DW) venom was applied to an ion exchange HPLC column (see Fig. 1, *legend*). The desired fraction containing DW13.3 was collected from 34 to 35.5 min, and pooled fractions were desalted without concentration. Subsequently, the material from ion exchange fractionation of 3360 μl of crude venom was applied to a Vydac C-18 HPLC column (300 Å, 5 μm, 22 × 250 mm; Nest Group, Southborough, MA) using a linear gradient program (A = 0.1% CF$_3$CO$_2$H; B = CH$_3$CN) with detection at 220 nM and a flow rate of 15 ml/min. The gradient was 23–30% B over 60 min, and the desired fraction containing DW13.3 was collected from 29 to 31 min. Pooled like fractions from individual runs were concentrated by lyophilization. Observed mass (ES-MS) = 8668 (calc. 8668.29).

DW13.3 (74 amino acids) was sequenced in native form and as its *S*-pyridylethylated derivative (providing the amino terminus of the peptide, ~ 50 amino acids). Pyridylethylated DW13.3 proved to be susceptible to enzymic attack, and a strategy with trypsin and Glu-C treatment was used to generate small peptide fragments amenable to amino acid sequencing. Glu-C digestion afforded, after separation by reverse-phase HPLC, six major fragments (34, 35, 42, 43.5, and 45 min) whose identity was confirmed by ES-MS and amino-terminal sequencing (Fig. 2). A second approach using trypsin digestion yielded five major fragments. Both digest patterns in concert with amino acid analysis (not shown) confirmed the assigned structure of the peptide (Table 1). Overall, the amino acid sequence of DW13.3 is distinct from that of other peptide calcium channel blockers, with the amino terminus of DW13.3 most closely related to curtotoxin

(~38%). Although DW13.3 is of a similar size and overall charge and shares 12 conserved cysteine residues with ω-Aga IIIA, these two toxins exhibit little sequence identity (<25%; Table 1).

DW13.3 potently blocks all four types of transiently expressed calcium channel. Bath application of DW13.3 (230 nM) produced a significant block of calcium channel currents transiently expressed in *X. laevis* oocytes. Four different types of calcium channel were investigated (α1A, α1B, α1C, and α1E), each coexpressed with α2δ and β1b subunits. DW13.3 produced a potent and reversible inhibition of all the calcium channels tested, although the degree of block and the rate of reversal of inhibition varied significantly among the subtypes (Fig. 3). Although the development of toxin block of the peak I_{Ba} (carried by 4 mM Ba^{2+} in all cases) was complete within 2 min of toxin application, the rate of recovery varied among the channel types. Three of the four calcium channels (α1B, α1C, and α1E) showed rapid and nearly complete reversal of toxin inhibition, recovering to ~70–80% of the control current within 4 min. In contrast, the recovery of α1A
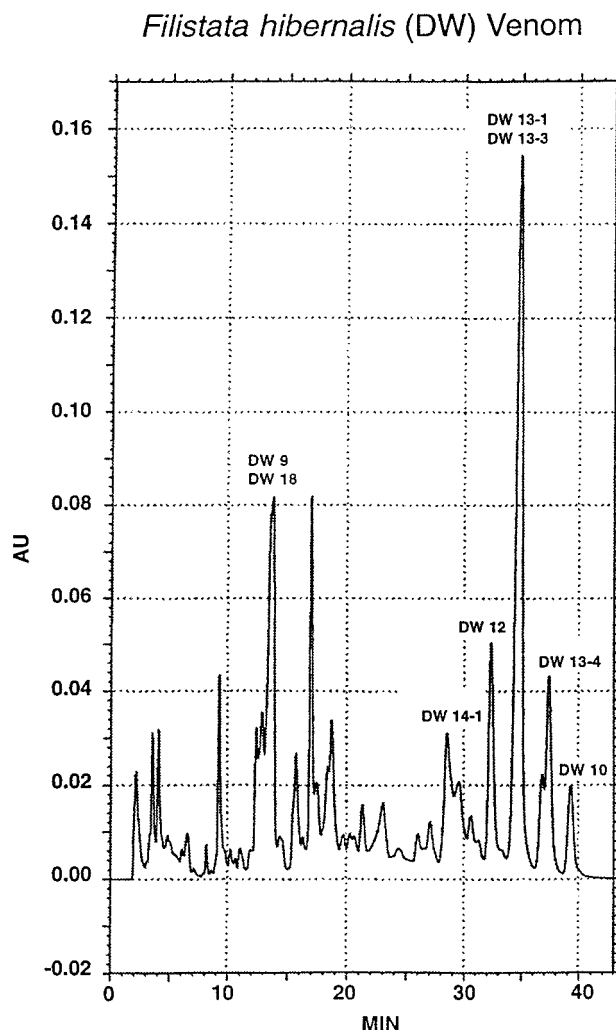
Filistata hibernalis (DW) Venom

Fig. 1. Preparative ion exchange chromatogram of DW13.3 isolation from crude venom. Crude *F. hibernalis* (DW) venom (~80 μl) was applied to a Poly LC polysulfoethyl aspartamide HPLC column (300 Å, 5 μm, 9.4 × 200 mm) using a triphasic linear gradient program (B = CH$_3$CN, C = 5 mM H$_3$PO$_4$/H$_2$O at pH 4.5, D = C + 1 M NaCl) with detection at 220 nm and a flow rate of 3.5 ml/min. The gradient was 20% B/80% C/0% D to 20% B/0% C/80% D over 45 min.

was markedly slower ($p < 0.01$), and in oocytes with particularly stable currents, it was still not complete after 20–25 min of perfusion with control solution (data not shown). The average time constants of recovery were 1506 ± 342, 77 ± 14, 66 ± 8, and 45 ± 5 sec for α1A, α1B, α1C, and α1E, respectively (7, 11, 7, and 6 determinations; Fig. 3, *inset*).

Block of the peak I_{Ba} by DW13.3 was potent, and substantial inhibition by nanomolar concentrations of the toxin was observed for all four calcium channels tested. However, fits of the data in the form of dose-response curves produced IC_{50} values that varied by up to 22-fold (4.3, 14.4, 26.8, and 96.4 nM for α1A, α1B, α1C, and α1E, respectively; Fig. 4). In each case, the dose-response relationship is well described assuming a 1:1 binding association of the toxin molecule with the channel (Hill coefficient = 1.0). Despite the finding that potency of DW13.3 inhibition was greatest for α1A, block of this channel saturated at only 60%, with fit of the data requiring the value for maximum block to be set considerably lower than 100% (i.e., incomplete block compared with 93% for α1C; Fig. 4, *current traces*).

Inhibition of α1B in HEK cells. In contrast to that for *X. laevis* oocytes, DW13.3 was found to be markedly more potent when tested on α1B calcium channel currents expressed in mammalian HEK cells (α1B HEK). Whole-cell currents were inhibited by concentrations of toxin as low as 300 pM, and analysis of the dose-response data yielded an IC_{50} value

of just 2.3 nM (Fig. 5, A and B). The rate of onset of block was rapid in α1B HEK cells, with maximal inhibition occurring within 1–2 min of application. However, the kinetics of toxin block were dissimilar compared with those observed in oocytes. The actions of DW13.3 were readily reversible in oocytes (Fig. 3), but there was little or no discernible recovery of α1B currents recorded in HEK cells within the 2–4-min recovery period (0–10%, four determinations; Fig. 5C). The relatively slow reversal of DW13.3 inhibition in α1B HEK cells yields an effective potency of this toxin 1 order of magnitude greater than that observed for the oocyte expression system (Fig. 5B).

Inhibition of N-type current in rat sympathetic neurons. DW13.3 block of native calcium currents (5 mM Ba, I_{Ba}) was studied in rat superior cervical ganglion neurons. These cells typically exhibit a large proportion of high threshold current that is carried through ω-CgTX GVIA-sensitive, N-type calcium channels (Boland *et al.*, 1994). In this study, saturating concentrations of nifedipine (10 μM) first were applied to block the L-type component of high threshold current in these cells (11 $\pm$ 1%, five determinations). Of the current that remained, 80.7 $\pm$ 1.2% (six determinations) could be blocked by saturating concentrations of ω-CgTX GVIA (3.2 μM). The current that was resistant to both nifedipine and ω-CgTX GVIA was also resistant to the P-type channel blocker ω-Aga IVA (200 nM).
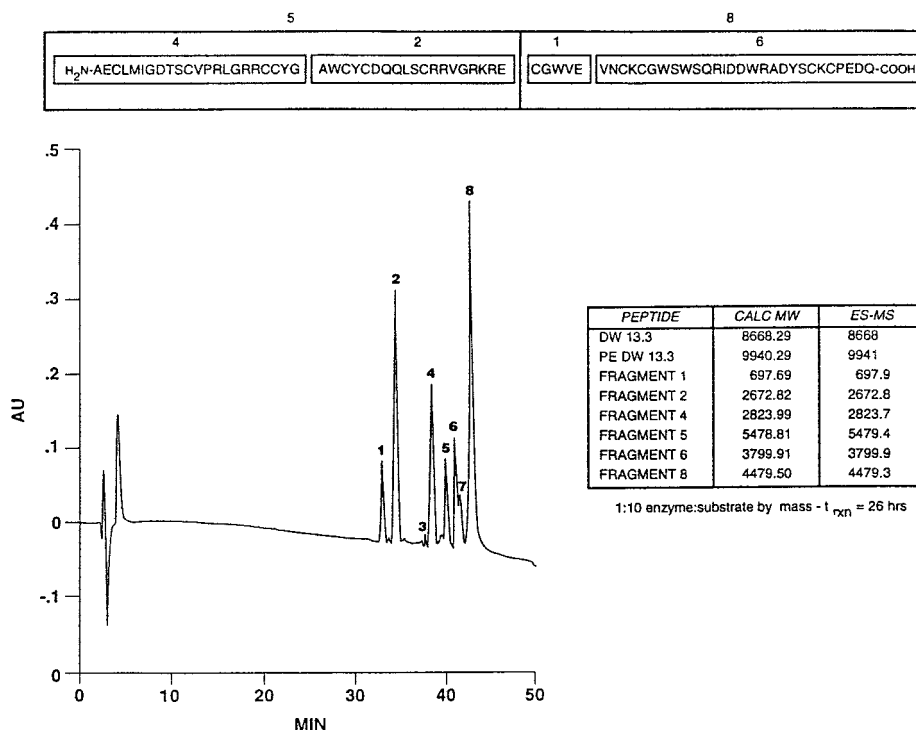

Fig. 2. ES analysis of peptide fragments generated in the Glu-C digest of pyridylethylated DW13.3. Pyridethylated DW13.3 (10 μg) in H_2O (10 μl) was combined with 100 μl of buffer (25 mM NH_4OAc, pH 4.0) and 10 μl of endopeptidase Glu-C solution (0.1 μg/ml) and maintained at 37° for 24 hr. The fragments were separated by reversed-phase HPLC (Vydac C-18, 300 Å, 5 μm, 4.6 $\times$ 250 mm) using a biphasic linear gradient program (A = 0.1% CF_3CO_2H; B = CH_3CN) with detection at 220 nm and a flow rate of 1 ml/min. The gradient was 0–30% B over 35 min and then 30–60% B over 25 min. Pyridylethylated derivative of DW13.3, suitable for amino-terminal sequencing, was prepared in the following manner: DW13.3 peptide (300 μg) was dissolved in 20 μl of buffer (1:3 ratio of 1 M Tris, pH 8.4, 4 mM EDTA-dibasic and 8 M guanidine hydrochloride), treated with 7.28 μl of a 10% v/v solution of 2-mercaptothanol in buffer, and kept in the dark at room temperature for 3 hr. The reaction then was treated with 11.19 μl of a 10% v/v solution of 4-vinylpyridine in buffer and kept at room temperature in the dark for an additional 18 hr. The reaction was diluted to 600 μl with 1% trifluoroacetic acid-H_2O and applied to an HPLC column (Vydac C-18, 4.6 $\times$ 250 mm), which was operated using a biphasic linear gradient program (A = 0.1% CF_3CO_2H, B = CH_3CN) with detection at 220 nm and a flow rate of 1.0 ml/min. The gradient was 0–30% B for 35 min and 30–60% B for 25 min. The desired fraction was collected from 34 to 35 min and concentrated by lyophilization. Approximate yield (based on amino acid analysis) was 194 μg. Observed mass was 9941 (calc. 9941.29).

TABLE 1

Sequences and cysteine alignment of DW 13.3 and other calcium channel toxins

Primary amino acid sequences of DW13.3 (Ahlijanian *et al.*, 1995); CT-III, a neurotoxic insecticidal polypeptide isolated from the venom of the funnel web spider *Hololena curta* (Stapleton *et al.*, 1990); ω-Aga IVa, a selective blocker of P-type Ca²⁺ channels isolated from the venom of the funnel web spider *Agelenopsis aperta* (Mintz *et al.*, 1992a, 1992b); ω-CgTX GVIA, a selective blocker of N-type Ca²⁺ channels isolated from the venom of the fish-hunting cone snail *Conus geographus* (Olivera *et al.*, 1984); ω-CTx MVIIC, a blocker of N- and P/Q-type Ca²⁺ channels whose structure was provided by a venom duct cDNA library (Hillyard *et al.*, 1992); and ω-Aga IIIA, a nonselective blocker of N-, L-, and P-type Ca²⁺ channels isolated from the venom of *Agelenopsis aperta* (Mintz *et al.*, 1991).

DW 13.3	AE	C LMIGDTS	C VPRLGRR	CC YGAW	C	Y C DQQLS	C RRVGRK RE	C GWVEVN	C K C GWSWSQRIDDWRADYS	C K C PEDQ–CO₂H
CT-III	AD	C VGDGQR	C ADWAGPY	CC SGYY	C	S C RSMPY	C R C	RSDS–CONH₂		
ω-Aga IVa	KKK	C IAKDYGR	C KWGGTP	CC RGRG	C	I C SIMGTN	C E C	KPRLIMEGLGLA–CO₂H		
ω-CgTX GVIA		C KSHγGSS	C SHγTSYN	CC RS	C	NHγYTKR	C Y–CONH₂			
ω-CTx MVIIC		C KGKGAP	C RKTMYD	CC SGS	C	GRRGK	C CONH₂			
ω-Aga IIIA	S	C IDIGGD	C DGEKDD	C Q	CC	RRNGY	C S C YSLFGYLKSG	C K C VVGTSAEFQGI	C RRKARQ	C YNSDPDK C ESHNKPKRR

A saturating concentration of DW13.3 (320 nM) eliminated $79 \pm 2\%$ (six determinations) of the nifedipine-resistant current in rat sympathetic neurons. Block was potent yet reversible, with substantial recovery observed after washing in control buffer for 3–4 min (Fig. 6A). Overall, DW13.3 inhibited the current in a 1:1 manner with an estimated IC_{50} value of 22 nM (based on a saturating block of 80%; Fig. 6B). Despite the fact that both DW13.3 and ω-CgTX GVIA blocked similar current components (~80%), application of DW13.3 (320 nM) in the presence of ω-CgTX GVIA (3.2 μM) produced an additional inhibition of the total nifedipine-resistant current ($14 \pm 2\%$, six determinations, $p < 0.01$; Fig. 6C), revealing not only substantial block of the N-type current but also additional inhibition of the unclassified residual current in these cells. Consequently, although DW13.3 inhibits a large proportion of the ω-CgTX GVIA-sensitive N-type current, block was not complete. A small yet significant amount of ω-CgTX GVIA-sensitive current persisted in the presence of DW13.3 (Fig. 6D). After pretreatment with 1 μM DW13.3, ω-CgTX GVIA produces an additional inhibition of $13 \pm 0.3\%$ (three determinations, $p < 0.001$). Based on the reciprocal blocking data obtained from adding DW13.3 before or after block by ω-CgTX GVIA, it can be calculated that saturating concentrations of DW13.3 (>320 nM) inhibit 84% of the N-type current and 73% of the small proportion of remaining, unclassified current in these cells (Fig. 6E).

Pretreatment by DW13.3 also affected the time course of subsequent inhibition by ω-CgTX GVIA. When used at a concentration of 3.2 μM, N-type channel inhibition by ω-CgTX GVIA in these cells is usually fast ($\tau_{on} = 4.8 \pm 0.6$ sec, three determinations) and irreversible. However, the rate of additional block by ω-CgTX GVIA was significantly slowed after pretreatment with DW13.3 ($\tau_{on} = 58 \pm 2$ sec, three determinations, $p < 0.001$; Fig. 6D). Previous experiments in this study show that high threshold currents in rat sympathetic
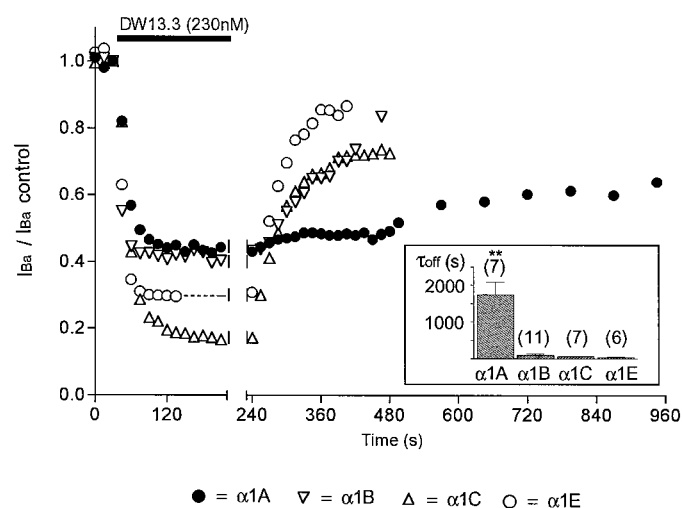

Fig. 3. Inhibition of transiently expressed calcium channels by DW13.3. Four different cloned calcium channels (α1A, ●; α1B, ▽; α1C, △; α1E, ○) were transiently coexpressed with α2δ and β1b subunits in *X. laevis* oocytes. Bath perfusion of a solution containing DW13.3 (230 nM) produced a rapid (within 2 min) and reversible inhibition of the peak Ba²⁺ current (4 mM Ba²⁺, $V_h = -100$ mV, $V_c = 0$, +10 mV, 400-msec step, activated every 15 sec), with α1A exhibiting a much slower rate of recovery from toxin block. *Inset*, comparison of the mean time constants ($\pm$ standard error) for recovery (τ_{off}) for the four different calcium channel clones. *Numbers in parentheses*, number of determinants for each sample. **, $p < 0.01$.

neurons recover from inhibition by DW13.3 (Fig. 6A). The slowed rate of ω-CgTX GVIA inhibition may be limited by the on- and off-rates of DW13.3 molecules dissociating from N-type channels. This raises the possibility that the additional decrease in current is not merely due to ω-CgTX GVIA block of a subpopulation of DW13.3-resistant N-type channels but rather represents the slow replacement of a reversible partial blocker by an irreversible toxin that completely blocks the channel. Previous studies have shown that ω-CgTX binding sites are located close to the external mouth of the channel pore (Ellinor *et al.*, 1994). The slowing of ω-CgTX GVIA-inhibition by DW13.3 therefore suggests that the two toxins may be directly competing for overlapping binding sites close to or at the mouth of the pore of the N-type channel and that DW13.3 produces incomplete occlusion of the channel. Alternatively, some form of competitive allosteric interaction could link two separate and distinct binding sites (Olivera *et*

al., 1994; Yan *et al.*, 1995). The difference in affinity of DW13.3 for N-type currents varies considerably between expression systems (Table 2), suggesting that cell-type-specific differences in post-translational modification may alter pharmacological properties.

Partial block of α1A in oocytes and of P-type currents in Purkinje neurons. Although the IC_{50} value for DW13.3 inhibition of the α1A calcium channel expressed in oocytes was 4.3 nM (Fig. 4), the highest saturating concentration of DW13.3 used in this study (1.15 μM) did not produce total block (68 ± 8%, three determinations). Fig. 7A shows that increasing concentrations of DW13.3 applied to a single oocyte produced a cumulative inhibition of the current that (in this case) saturated at ~55%. The dose-response data for α1A are well described assuming a Hill coefficient of 1.0, consistent with 1:1 binding of the toxin molecule with the calcium channel. Nevertheless, fit of the data did require a model based on incomplete block (even if block was not assumed to occur in a unitary manner; i.e., when the Hill coefficient was not fixed at 1.0).

In confirmation of the stoichiometry of this interaction, the rate of toxin block should be linearly dependent on the toxin concentration. The time course of onset for DW13.3 block for α1A could be fitted well with a single exponential (Fig. 7B), and the plot of $1/\tau_{on}$ exhibited a linear concentration dependence as would be expected from a 1:1 interaction (Fig. 7C). The slope corresponded to a binding rate constant (k_{on}) of 2.5×10^{-4} nM^{-1} sec^{-1}, and the estimated K_d value was 7.7 nM. For comparison, the data also was fitted with a linear function in which the y-intercept was fixed to the reciprocal
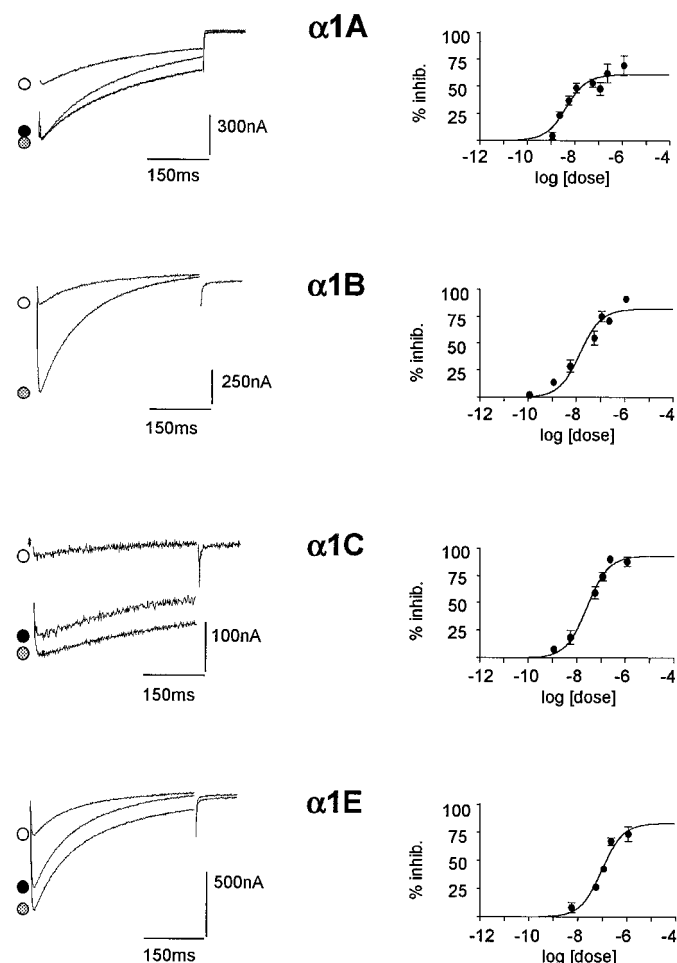

Fig. 4. Dose dependence of DW13.3 inhibition of expressed calcium channels. *Current traces*, DW13.3 inhibition of transiently expressed peak control Ba^{2+} currents (α1A, α1B, α1C, and α1E) by a saturating concentration of DW13.3 (1.15 μM; ◉, control; ○, DW13.3; ●, recovery). *Opposite*, dose-response data are summarized for all four calcium channel types. Data points represent mean ± standard error values (2–10 determinations) of the percent current inhibited after the perfusion of DW13.3 (2–16 min). Solid line fits were made to the following equation and assumed 1:1 binding of the toxin with the channel: $Y = \max/[1 + (IC_{50}/[toxin])]$, where max is maximum inhibition. Barium currents (4 mM) were activated every 15 sec with a 400-msec step depolarization from −100 mV to 0 or −10 mV. DW13.3 inhibition of α1A was the most potent ($IC_{50} = 4.3$ nM) yet remained incomplete.
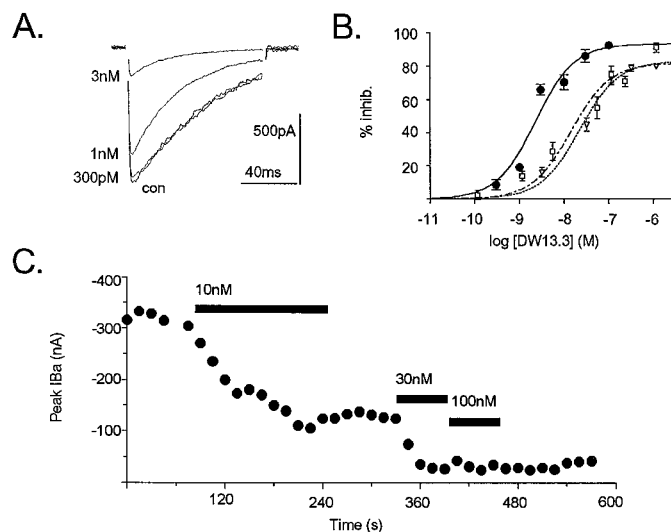

Fig. 5. DW13.3 inhibition of α1B channels expressed in HEK cells. A, Currents were recorded from a single cell exposed to progressive applications of increasing toxin concentrations (300 pM, 1 nM, 3 nM). Currents were activated every 15 sec by 100-msec step depolarizations to +10 mV from a holding potential of −100 mV. B, Dose-response relation for α1B currents recorded in HEK cells (*solid line*; $IC_{50} = 2.3$ nM). Also included for comparison are data points and fits obtained for α1B currents expressed in *X. laevis* oocytes (*intermittent broken line*; $IC_{50} = 14.4$ nM) and the nifedipine-resistant (mainly N-type) currents recorded in rat sympathetic neurons (*short broken line*; $IC_{50} = 22$ nM). All data point represent mean values (± standard error, 2–9 determinations) of the percent inhibition of the control current and were fitted with the following equation assuming 1:1 binding of the toxin with the channel: $Y = \max/[1 + (IC_{50}/[toxin])]$. C, Time course showing irreversible saturating block of the α1B current recorded in HEK cells ($V_h = -100$ mV, $V_c = 0$ mV, 100-msec step depolarizations activated every 15 sec).
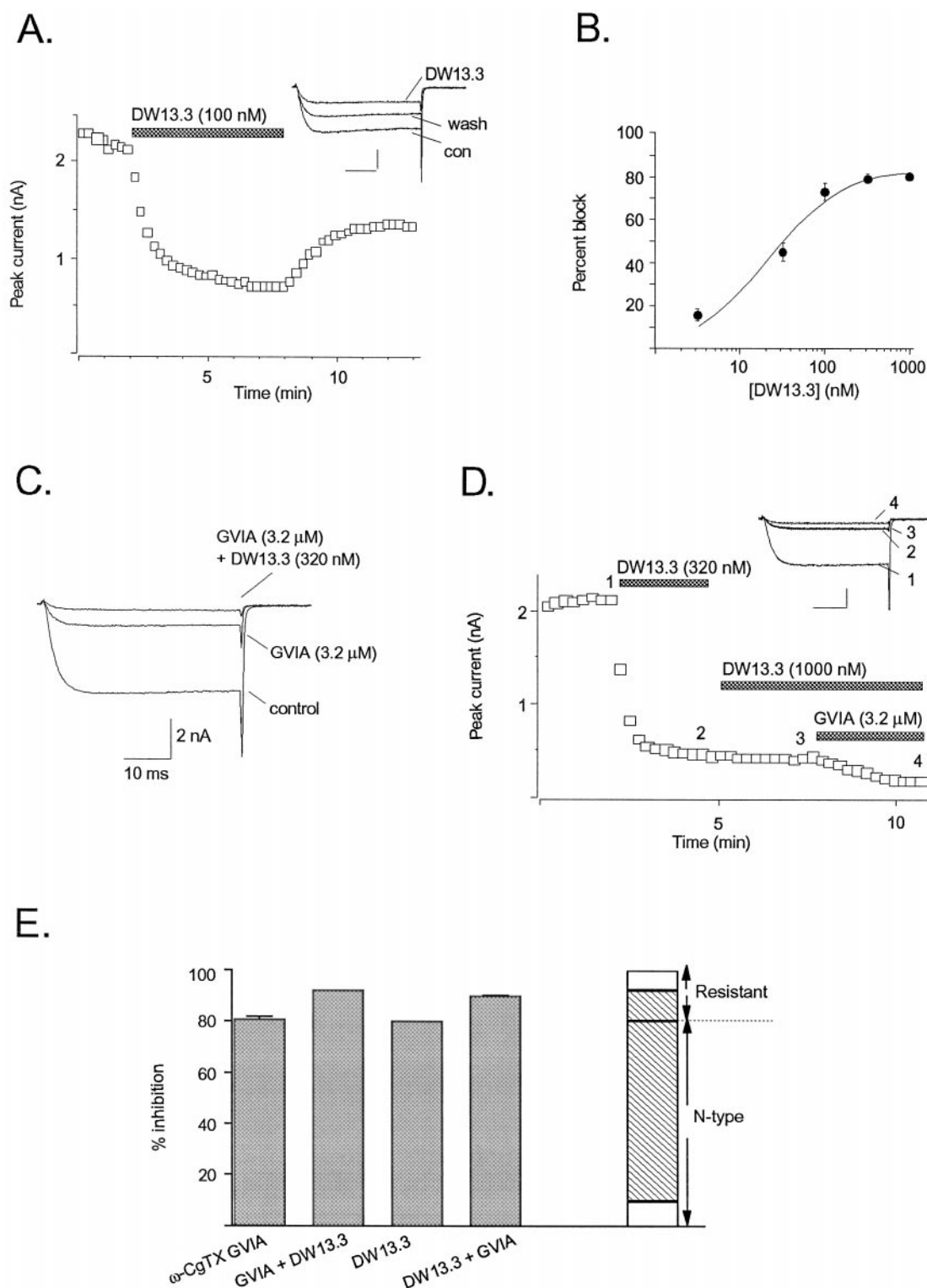
Fig. 6. DW13.3 block of ω-CgTX GVIA-sensitive, N-type current in rat sympathetic neurons. Currents were activated every 15 sec by a 35-msec step depolarization from -90 mV to $+10$ mV after the application of 10 μM nifedipine to block L-type current. A, Time course taken from a cell showing the reversible inhibition of nifedipine-insensitive, high threshold I_{Ba} (5 mM Ba^{2+}) by DW13.3 (100 nM). *Inset*, current trace scale bar = 1 nA and 10 msec. B, Concentration dependence of DW13.3 inhibition of the nifedipine-resistant I_{Ba}. Data points reflect mean $\pm$ standard error of two to nine determinations. Solid line fit was made assuming a 1:1 binding association of the toxin with the channel and is based on 80% saturating block of the remaining current. C, Current traces showing additional block of high threshold nifedipine-resistant current by DW13.3 in the presence of ω-CgTX GVIA. D, Preapplication of DW13.3 interferes with additional block by ω-CgTX GVIA. Peak currents were recorded under control conditions (*inset*, current trace 1) and during the sequential addition of DW13.3 (320 nM and 1 μM; current traces 2 and 3, respectively) and ω-CgTX GVIA (3.2 μM; current trace 4; scale bar = 1 nA and 10 msec). Rate of onset and efficacy of additional block by ω-CgTX GVIA is significantly reduced in the presence of DW13.3. E, Bar graph summarizing toxin-sensitive components of high threshold, non-L-type current in rat sympathetic neurons. Saturating concentrations of DW13.3 ($>$320 nM) inhibit 83% of the N-type current and 73% of the remaining nifedipine-resistant current (mean $\pm$ standard error of three to six determinations).

value for τ_{off} obtained independently from wash-off values from the same sets of data ($k_{on} = 2.6 \times 10^{-4}$ nM^{-1} sec^{-1}, K_d = 2.6 nM). Both fits produced affinity values that were similar to the IC$_{50}$ value obtained from the fit of the dose-response curve (4 nM) and the mean K_d value calculated from the toxin on-rate and off-rate time constants derived from individual cells (4.4 ± 1.8 nM, six determinations; see Table 2).

The effect of DW13.3 was also studied on the ω-Aga IVA-sensitive (P-type) current in rat cerebellar Purkinje neurons. Although there has been considerable speculation as to whether the α1A subunit might encode the P- and/or Q-type channel or a subfamily (O/P/Q) of calcium channels, α1A and P-type channels share significant structural and functional properties (Adams *et al.*, 1993a; Stea *et al.*, 1994; Randall and Tsien, 1995). P-type currents (5 mM Ba^{2+}) were recorded in the presence of 10 μM nifedipine to suppress the small fraction of L-type Ca channels in these cells. At saturating concentrations, both ω-CTx MVIIC (5 μM) and ω-Aga IVA (200 nM) effectively blocked 94% of the nifedipine-resistant (P-type) current in Purkinje neurons (Fig. 8, A and D). Inhibition by ω-Aga IVA (200 nM) was readily reversed by applying a series of depolarizing prepulses to +75 mV in the presence of control buffer (Fig. 8A; Mintz *et al.*, 1992a, 1992b). In contrast, saturating concentrations of DW13.3 (32–100 nM) produced only a partial (76 ± 2%, 11 determinations) inhibition of the ω-Aga IVA-sensitive (P-type) current (Fig. 8, B and D). Onset of DW13.3 block was rapid ($\tau = 27$ sec) compared with ω-Aga IVA ($\tau = 68$ sec) and could not be reversed by washing (>6 min) or by the application of depolarizing prepulses.

A comparison between additional block by ω-CTx MVIIC and ω-Aga IVA revealed notable differences in the effectiveness of DW13.3 at exclusion of P-type channel ligands from their channel binding sites. Partial inhibition by DW13.3 (32 nM) prevented complete block by ω-CTx MVIIC but not by ω-Aga IVA. The proportion of DW13.3-resistant P-type current remained unchanged after the application of ω-CTx MVIIC (78 ± 1%, four determinations). In contrast, ω-Aga IVA exerted an additional block, such that combined inhibition by DW13.3, ω-CTx MVIIC, and ω-Aga IVA was 98 ± 3% (three determinations; Fig. 8, B–D). Previous studies have identified a lack of exclusion between ω-Aga IVA and subsequent binding of the pore blocker ω-CTx MVIIC in Purkinje neurons (McDonough *et al.*, 1995). Because inhibition of DW13.3 only interfered with block by ω-CTx MVIIC and not by ω-Aga IVA, this suggests that DW13.3 interacts with a binding site that overlaps with that of ω-CTx MVIIC in close proximity or within the pore of the channel.

DW13.3 inhibition of pharmacologicaly unclassified components of native calcium channel currents. In addition to inhibiting components of pharmacologicaly defined high threshold current, DW13.3 exhibited a potent block of a number of other uncharacterized current types. A considerable proportion (~70%) of the non-L-, non-N-, non-P/Q-type current in rat sympathetic neurons was sensitive to block by saturating concentrations of DW13.3 (>320 nM; see above). A number of studies have suggested a correlation between the α1E channel and a component of rapidly inactivating current in cerebellar granule neurons that is resistant to L-, N-, and P/Q-type channel blockers (R-type current) (Zhang *et al.*, 1993; Randall and Tsien, 1995). Initial experiments on expressed channels revealed a potent yet partial block of the α1E channel (Table 2). The actions of DW13.3 on the resistant component of current were investigated in cerebellar granule neurons. A combination of nifedipine (10 μM), ω-CgTX GVIA (1 μM), and ω-CTx MVIIC (5 μM) was used to block the L-, N-, and P/Q-type channels respectively. In this study L-, N-, and P/Q-type current represented 49 ± 3% (10 determinations) of the total whole-cell current. Fig. 9 shows the results of the coapplication of these three channel blockers followed by the effects of subsequent addition of DW13.3 (100 nM). DW13.3 rapidly (within 1–2 min) blocked 82 ± 4% (four determinations) of the remaining resistant current. In contrast with α1E, inhibition did not seem to reverse after washing for 5 min with control solution (three determinations, data not shown). Preliminary experiments carried out on whole-cell currents in GH3 cells revealed that this T-type current showed little or no sensitivity to a concentration of DW13.3 that significantly reduced the L-type current in these cells (230 nM; data not shown).

Discussion

DW13.3 inhibition of L-, N-, and P/Q-type currents. This study shows that DW13.3 exhibits a potent block of calcium channel currents recorded in a variety of cultured mammalian cells and exogenous expression systems (summarized in Table 2). The dose-response data obtained for each of the calcium channel clones indicate that the toxin binds in a 1:1 manner, producing differing degrees of block at saturating concentrations. Of the four clones examined in this study, DW13.3 inhibition of the α1C L-type channel was most complete. Previously, DW13.3 had been shown to dis-

TABLE 2
Summary of IC$_{50}$, K_d, τ_{off}, and maximum percent inhibition values

	α1A	α1B (oocyte)	α1B (HEK)	α1C	α1E	DHP-resistant I_{Ba} (sympathetic neurons)	P/Q I_{Ba} (Purkinje neurons)
IC$_{50}$ (nM)[a]	4.3	14.4	2.3	26.8	96.4	22	N.D.
K_d (nM)[b]	4.4 ± 1.8 (6)	19 ± 6 (5)	N.D.	75 ± 20 (6)	52 ± 15 (5)	48[c]	N.D.
τ_{off} (sec)$^{-1}$[b]	1506 ± 342 (7)	77 ± 14 (11)	N.D. (irreversible)	66 ± 7 (6)	44 ± 5 (6)	N.D. (partially reversible)	N.D. (irreversible)
Maximum inhibition,[a] (%)	60	82	94	93	83	80 (N-type = 83)[d]	76[e]

[a] Values derived from fits of dose-response data.
[b] Mean values (± Standard error) derived from kinetic data (τ_{on} and τ_{off}) obtained from individual cells (numbers in parentheses indicate number of cells included in each sample).
[c] Estimated from a linear fit of the kinetic data.
[d] Calculated from the proportion of ω-CgTX GVIA-sensitive current blocked by DW13.3.
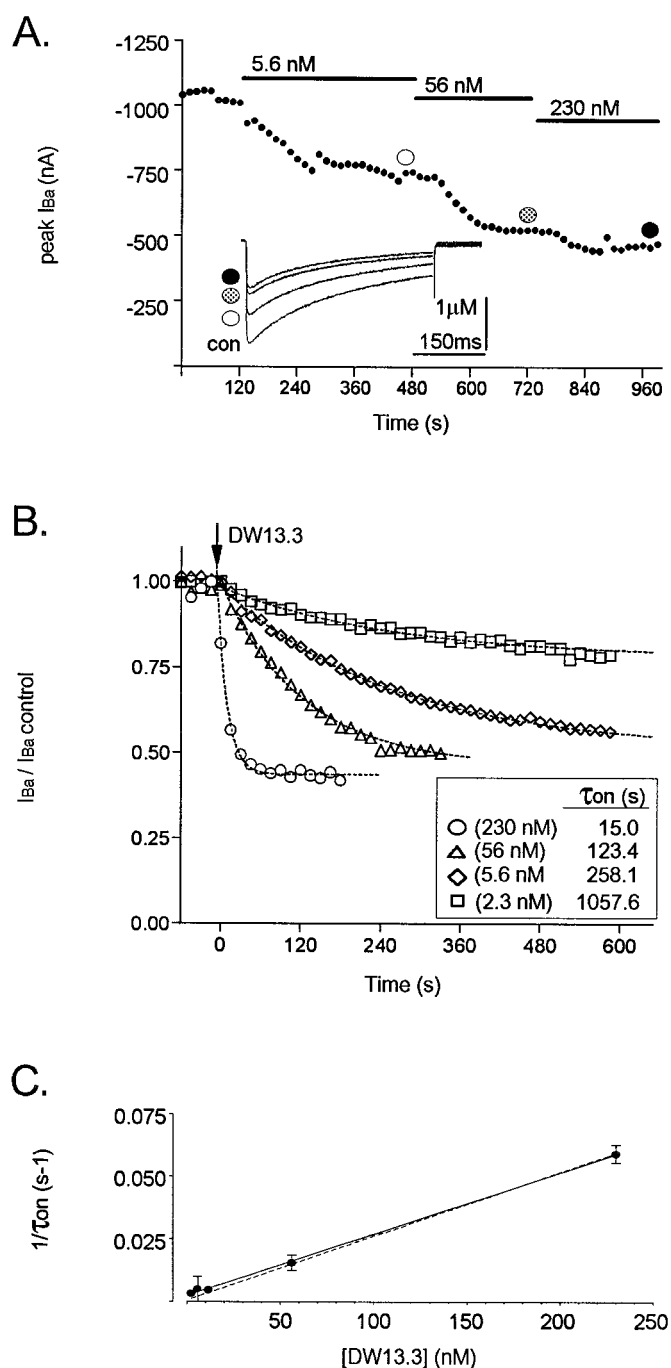[e] Maximum block with saturating concentrations of DW 13.3 (32-100 nM).

Fig. 7. Partial inhibition of α1A expressed in *X. laevis* oocytes. A, Time course showing three sequential applications of increasing concentrations of DW13.3 on the same oocyte. Currents were elicited every 15 sec by 400-msec step depolarizations to +10 mV from a holding potential of −100 mV. *Inset*, current traces were taken from the same cell at points indicated (*con*, control, ○, 5.6 nM, ◉, 56 nM, ●, 230 nM). Inhibition by DW13.3 saturates at <100% block. B, Time course of block in four different oocytes exposed to 2.3, 5.6, 56, and 230 nM DW13.3. Barium currents (4 mM) were activated every 15 sec with 400-msec step depolarizations from −100 mV to 0 or +10 mV. Currents were normalized to the control current amplitude recorded just before toxin application (↓). *Dotted lines*, fits of single exponentials decaying to a plateau (τ_{on}). C, Dependence of $1/\tau_{on}$ on [DW13.3]. Values are mean ± standard error of four to seven determinations. Solid line fit was made to the following equation: $1/\tau_{on} = k_{on} \cdot [DW13.3] + k_{off}$, where k_{on} is 0.000249 ($nM^{-1}\ sec^{-1}$), k_{off} is 0.00192 (sec^{-1}), and K_d is 7.7 nM. *Dotted line*, a fit in which the y-intercept was fixed to the mean value obtained from kinetic analysis of the toxin off-rate calculated from individual cells (τ_{off} = 1506 ± 342 sec, seven determinations; k_{off} = 0.000595 sec^{-1}, k_{on} = 0.000256 $nM^{-1}\ sec^{-1}$, and K_d = 2.6 nM).

criminate between 1,4-dihydropyridine-sensitive L-type currents recorded from rat cerebellar granule cells and a rat aortic cell line (A7R5; IC_{50} = 0.4 nM and 16 nM, respectively; Ahlijanian *et al.*, 1995). When compared, DW13.3 inhibition of the rat cerebellar granule cell L-type current was by far the most potent observed to date. This 20-fold difference in affinity between L-type channel isoforms may reflect regional differences in the expression of α1C and α1D L-type channels and provide a means of discriminating between L-type currents in neuronal versus smooth muscle preparations. A direct comparison of the affinity of DW13.3 for heterologously expressed α1C and α1D subunits may help to explain these observed differences in potency.

Initial studies of DW13.3 inhibition of α1B N-type currents showed a potent and reversible block that saturated at just <100%. The slower rate of recovery from block of α1B current expressed in HEK cells produced a significantly higher affinity of block in this preparation than for rat sympathetic neurons or *X. laevis* oocytes. Differences in glycosylation of external channel residues or small conformational differences in the different cell types may have a profound effect on the ability of the toxin to remain bound to the channel.

In contrast to the other channel types, a considerable proportion of α1A P/Q-type current (~40%) remained insensitive to block by saturating concentrations of DW13.3. The dose-response data and binding kinetics of inhibition of α1A currents are well described assuming a 1:1 binding relationship of the toxin for the channel (as are the other channels, α1B, α1C, and α1E). Complementary experiments carried out on P-type currents in Purkinje neurons revealed a similar, although not identical, profile of block. DW13.3 acted as a high affinity partial blocker (~75%) of the ω-Aga IVA-sensitive P-type current in these cells. Block was slow to reverse and prevented inhibition by ω-CTx MVIIC yet did not exclude additional inhibition by ω-Aga IVA. If block by DW13.3 discriminates among different isoforms of the P-type calcium channel, a subpopulation of DW13.3-resistant P-type channels would be expected to remain sensitive to block by ω-CTx MVIIC. The total exclusion of ω-CTx MVIIC block by DW13.3 therefore suggests that DW13.3 is acting on all P-type calcium channels in a similar manner to partially reduce calcium influx rather than leaving a proportion of channels unaffected by block.

DW13.3 inhibition of non-L-, -N-, and -P/Q-type current. Initial experiments on expressed channels revealed a potent yet partial block of the α1E channel. A comparable component of endogenous α1E current has yet to be unequivocally identified because no selective pharmacological agent for this channel has been described. A number of studies have suggested a correlation between the α1E channel and a component of the residual current in cerebellar granule neurons (Zhang *et al.*, 1993; Randall and Tsien, 1995); however, the biophysical and pharmacological properties of these currents do not match "R-type" currents (compare Soong *et al.*, 1993, and Bourinet *et al.*, 1996). In this study, 100 nM DW13.3 (a concentration that produces maximal block of α1E currents) was found to irreversibly inhibit a significant proportion (~80%) of the resistant current in cerebellar granule neurons. In addition, a proportion (~20%) of the resistant current also persisted in the presence of all four blockers. Because by definition this current is isolated by virtue of exclusion to block by nifedipine, ω-CgTX GVIA, and ω-CTx

MVIIC, it remains to be elucidated whether block by DW13.3 represents complete inhibition of an additional subpopulation of previously uncharacterized channels or partial block of the resistant current.

Structural considerations for DW13.3. DW13.3 shares very little structural identity with other calcium channel peptide toxins (Table 1). The broad specificity of DW13.3 inhibition and its varied blocking efficacy are very similar to those of ω-Aga IIIA, a peptide spider toxin isolated from the venom of the funnel web spider *A. aperta* (Cohen *et al.*, 1992; Ertel *et al.*, 1994; Mintz, 1994; Ahlijanian *et al.*, 1995). However, these two toxins lack any form of sequence homology. In fact, the amino terminus of DW13.3 is most closely aligned with the μ-agatoxin family. The first 33 residues of curtotoxin (CT-III) (Stapleton *et al.*, 1990), which has the same cysteine topology as the ω-Aga IV toxins, are 38% identical with amino acids on the amino terminus of DW13.3.

Despite their lack of sequence identity, both DW13.3 and ω-Aga IIIA have a comparable overall positive charge and high density core of 12 cysteine residues in their 74- and 76-amino acid polypeptide frameworks. As is the case with other ion channel toxins, the six disulfide bridges of these toxins likely play a key role in establishing and maintaining their three-dimensional protein structure, as well as constraining amino acids into a defined molecular architecture (Olivera *et al.*, 1990). The lack of sequence homology between these two toxins suggests that the interaction of DW13.3 with the calcium channel may be determined by the overall tertiary structure and charge distribution of the folded protein as opposed to regions of more specific residue/residue interactions. In addition, preliminary experiments carried out in this study on whole-cell currents in GH3 cells revealed that T-type current showed little or no sensitivity to a concentration of DW13.3 that significantly reduced the L-type current in these cells (230 nM; data not shown). This unique resistance of T-type currents (as for ω-Aga IIIA; Cohen *et al.*, 1992; Mintz, 1994) suggests that the outer pore region of the T-type channel has a different structure among calcium channels, preventing access of DW13.3 to a binding site that seems to be relatively conserved in other calcium channels.

Where does DW13.3 act?. Although the specificity of P- and N-type calcium channel toxins for their respective molecular targets has shed some light on which structural features of the peptide toxins are important for channel inhibition, these standards alone are not sufficient for solving this problem (Adams *et al.*, 1993b; Omecinsky *et al.*, 1996). Toxins such as DW13.3 are structurally distinct yet target multiple calcium channel subtypes. Extreme degeneracy in the sequences of different N-type specific ω-conotoxins has already been described (Olivera *et al.*, 1990). ω-Conotoxin binding to N-type channels is thought to involve interaction of the conserved tertiary structure of the peptides with a "macro" li-
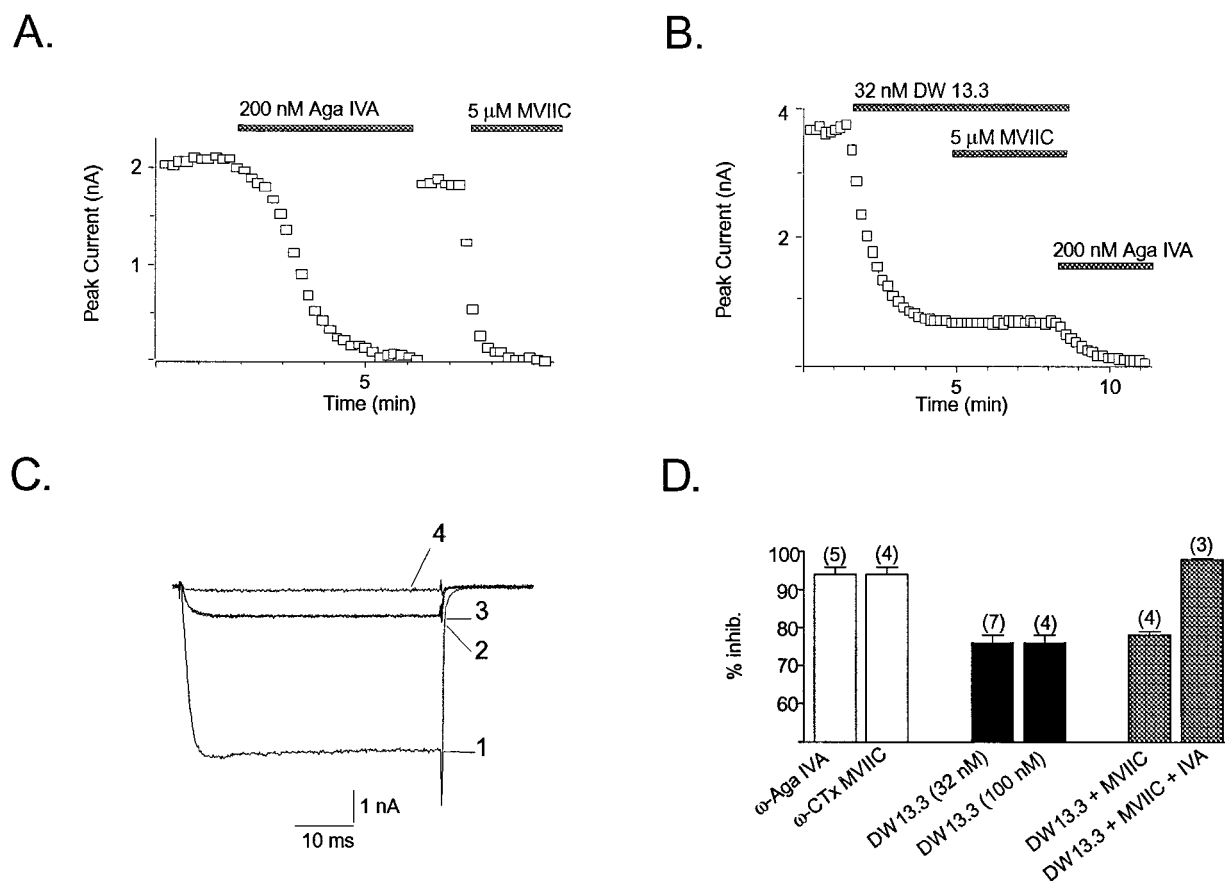

Fig. 8. DW13.3 partially inhibits the P-type current in Purkinje neurons but does not occlude complete block by ω-Aga IVA. A, Both ω-Aga IVA and ω-CTx MVIIC effectively inhibit all P-type current present in Purkinje neurons. B, Partial block by saturating concentrations of DW13.3 prevents additional inhibition by ω-CTx MVIIC but not by ω-Aga IVA. C, Current traces showing the progressive block of the control P-type current (*1*) after the application of 32 nM DW13.3 (*2*) followed by 5 μM ω-CTx MVIIC (*3*) and 200 nM ω-Aga IVA (*4*). D, Data showing that DW13.3 selectively occludes ω-CTx MVIIC but not ω-Aga IVA from binding to P-type calcium channels. Nifedipine (10 μM) was present throughout all these experiments. Peak inward currents (5 mM Ba^{2+}) were elicited by 35-msec step depolarizations to −20 mV from a holding potential of −80 mV.

gand binding site. The specificity of binding is determined by a number of smaller "micro" interactions that are specific to the residues of each individual toxin. The macrobinding site is able to tolerate the hypervariable domains of each different toxin as they are constrained by the disulfide bonds formed between conserved residues forming a common overall three dimensional structure (Olivera *et al.*, 1990, 1991). The "macrosite hypothesis" has also been proposed for a number of other peptide toxins exhibiting a broad specificity for calcium channels (Olivera *et al.*, 1994). Both ω-Aga IIIA and ω-CTx MVIIC inhibit a number of different calcium channels with differing binding affinities and blocking efficacies (Hillyard *et al.*, 1992; Mintz, 1994; Stea *et al.*, 1994; Randall and Tsien, 1995).

Data obtained in this study for N-type calcium channels in rat sympathetic neurons suggest that pretreatment with DW13.3 alters block by ω-CgTX GVIA. Moreover, block of whole-cell calcium channel currents by ω-CTx MVIIC is prevented by the prior application of DW13.3. However, DW13.3 does not bind to a site that overlaps with that defined by ω-Aga IVA in that DW13.3-resistant P-type current remains available for block by the subsequent addition of ω-Aga IVA. Differential exclusion and partial block by DW13.3 are consistent with the toxin binding close to the pore of the channel at a site that overlaps that occupied by the pore blockers ω-CgTX GVIA (N-type) and ω-CTx MVIIC (N- and P/Q-type) yet is distinct from the region of the P/Q-type channel that interacts with ω-Aga IVA.

DW13.3 is a large, rigid peptide, and the fact that it inhibits a variety of currents with relatively high affinity may well reflect a large degree of structural conservation within the outer pore regions of the different calcium channels. The general inhibition of calcium channel currents (with the notable exception of T-type current) coupled with the distinct channel-specific efficacy of DW13.3 therefore should make this toxin useful in determining both the similarities and differences present within the different subtypes of calcium channels. Any subtype-specific difference in the channel residues available for toxin binding might be expected to create significant differences in the rate and degree of maximum block, such as the partial and relatively irreversible block of α1A by DW13.3 seen in this study.

In summary, DW13.3 is a potent calcium channel blocker that may have use in defining the role of calcium channels that are insensitive to currently described toxin probes. The contribution of DW13.3 to the overall issue of molecular recognition, however, must await mapping and structural studies.

Acknowledgments

Fig. 9. DW13.3 inhibits residual current in cerebellar granule neurons. A, Current traces from a single cerebellar granule neuron show additional inhibition of the resistant current by DW13.3 (100 nM) after inhibition of L-, N-, and P/Q-type currents. B, Average time course from three cells. DW13.3 (100 nM, ●) produced a significant inhibition of the resistant current remaining in the presence of saturating concentrations of L-, N-, and P/Q-type channel blockers nifedipine (10 μM), ω-CgTX GVIA (1 μM), and ω-CTx MVIIC (5 μM) compared with control (○). Peak currents (10 mM Ba^{2+}) were activated every 15 sec by 35-msec step depolarizations to either 0 or +10 mV from a holding potential of −100 mV.

References

Adams ME, Mintz IM, Reily MD, Venkataraman T, and Bean BP (1993a) Structure and properties of ω-agatoxin IVB, a new antagonist of P-type calcium channels. *Mol Pharmacol* **44:**681–688.

Adams ME, Myers RA, Imperial JS, and Olivera BM (1993b) Toxityping rat brain calcium channels with ω-toxins from spider and cone snail venoms. *Biochemistry* **32:**12566–12570.

Ahlijanian MK, Artman LD, Stea A, Williams RD, Lanyon LF, Welch MJ, Heck S, Ronau R, Snutch TP, and Volkmann RA (1995) DW13.3, a peptide toxin from the spider *Filistata*, is a novel calcium channel blocker. *Soc Neurosci Abstr* **21:**140.1.

Bascur L, Yevenes I, and Adrian H (1980) An electric method to obtain *Loxosceles* spider venom. *Toxicon* **18:**224.

Bean BP (1989) Classes of calcium channels in vertebrate cells. *Annu Rev Physiol* **51:**367–384.

Boland LM, Morrill JA, and Bean BP (1994) ω-Conotoxin block of N-type calcium channels in frog and rat sympathetic neurons. *J Neurosci* **14:**5011–5027.

Bourinet E, Zamponi GW, Stea A, Soong TW, Lewis BA, Jones LP, Yue DT, and Snutch TP (1996) The $α_{1E}$ calcium channel exhibits permeation properties similar to low-voltage-activated calcium channels. *J Neurosci* **16:**4983–4993.

Charnet P, Bourinet E, Dubel SJ, Snutch TP, and Nargeot J (1994) Calcium currents recorded from a neuronal $α_{1C}$ L-type calcium channel in *Xenopus* oocytes. *FEBS Lett* **344:**87–90.

Cohen CJ, Ertel EA, Smith MM, Venema VJ, Adams ME, and Leibowitz MD (1992) High affinity block of myocardial L-type calcium channels by the spider toxin ω-agatoxin IIIA: advantages over 1,4-dihydropyridines. *Mol Pharmacol* **42:**947–951.

Dubel SJ, Starr TB, Hell J, Ahlijanian MK, Enyeart JJ, Catterall WA, and Snutch TP (1992) Molecular cloning of the α-1 subunit of an ω-conotoxin-sensitive calcium channel. *Proc Natl Acad Sci USA* **89:**5058–5062.

Ellinor PT, Zhang J-F, Horne WA, and Tsien RW (1994) Structural determinants of the blockade of N-type calcium channels by a peptide neurotoxin. *Nature (Lond)* **372:**272–275.

Ertel EA, Warren VA, Adams ME, Griffin PR, Cohen CJ, and Smith McM (1994) Type III ω-agatoxins: a family of probes for similar binding sites on L- and N-type calcium channels. *Biochemistry* **33:**5098–5108.

Fox AP, Nowycky MC, and Tsien RW (1987) Kinetic and pharmacological properties distinguishing three types of calcium currents in chick sensory neurons. *J Physiol (Lond)* **394:**149–172.

Hillyard DR, Monje VD, Mintz IM, Bean BP, Nadasdi L, Ramachandran J, Miljanich G, Azimi-Zoonooz A, McIntosh JM, Cruz LJ, Imperial JS, and Olivera BM (1992)
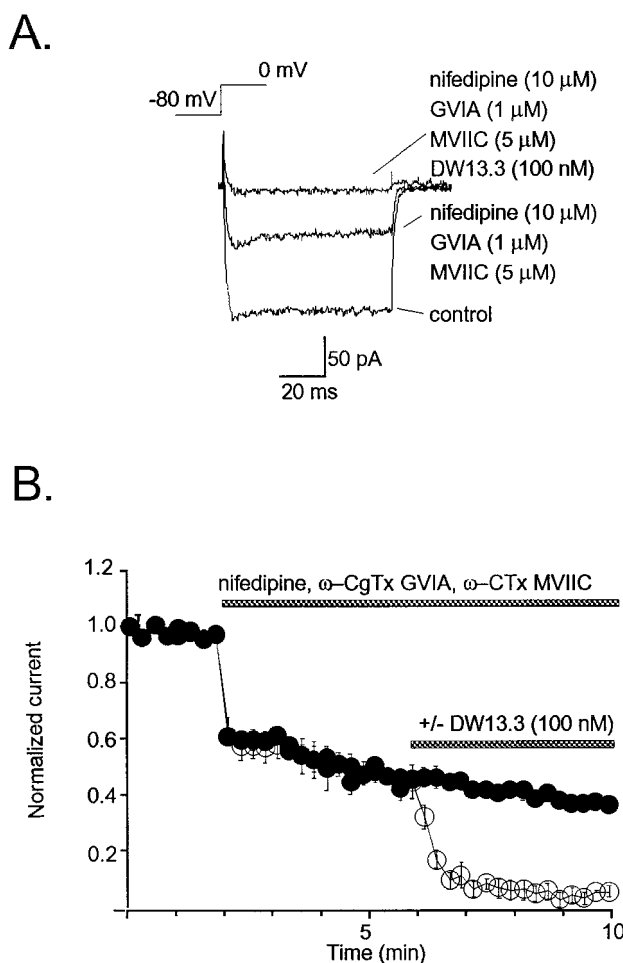
A new *Conus* peptide ligand for mammalian presynaptic Ca^{2+} channels. *Neuron* **9:**69–77.

McDonough SI, Mintz IM, and Bean BP (1995) ω-Conotoxin MVIIC block of N-type and P-type calcium channels: interactions with other toxins. *Soc Neurosci Abstr* **21:**140.9.

Mintz IM (1994) Block of Ca channels in rat central neurons by the spider toxin ω-Aga IIIA. *J Neurosci* **14:**2844–2853.

Mintz IM, Adams ME, and Bean BP (1992a) P-type calcium channels in rat central and peripheral neurons. *Neuron* **9:**85–95.

Mintz IM, Venema VJ, Adams ME, and Bean BP (1991) Inhibition of N- and L-type Ca^{2+} channels by the spider venom toxin ω-Aga-IIIA. *Proc Natl Acad Sci USA* **88:**6628–6631.

Mintz IM, Venema VJ, Swiderek KM, Lee TD, Bean BP, and Adams ME (1992b) P-type channels blocked by the spider toxin ω-Aga IVA. *Nature (Lond)* **355:**827–829.

Mori Y, Friedrich T, Kim MS, Mikami A, Nakai J, Ruth P, Bosse E, Hofmann F, Flockerzi V, Furuichi T, Mikoshiba K, Imoto K, Tanabe T, and Numa S (1991) Primary structure and functional expression from complementary DNA of a brain calcium channel. *Nature (Lond)* **350:**398–402.

Olivera BM, McIntosh JM, Cruz LJ, Luque FA, and Gray WR (1984) Purification and sequence of a presynaptic peptide toxin from *Conus geographus* venom. *Biochemistry* **23:**5087–5090.

Olivera BM, Miljanich GP, Ramachandran J, and Adams ME (1994) Calcium channel diversity and neurotransmitter release: the ω-conotoxins and ω-agatoxins. *Annu Rev Biochem* **63:**823–67.

Olivera BM, Rivier J, Clark C, Ramilo CA, Corpuz GP, Abogadie FC, Mena EE, Woodward SR, Hillyard DR, and Cruz LJ (1990) Diversity of *Conus* neuropeptides. *Science (Washington DC)* **249:**257–263.

Olivera BM, Rivier J, Scott JK, Hillyard DR, and Cruz LJ (1991) Conotoxins. *J Biol Chem* **266:**22067–22070.

Omecinsky DO, Holub KE, Adams ME, and Reily MD (1996) Three-dimensional structure analysis of μ-agatoxins: further evidence for common motifs among neurotoxins with diverse ion channel specificities. *Biochemistry* **35:**2836–2844.

Perez-Reyes E, Cribbs LL, David A, Lacerdd AE, Boudary J, Williamson MP, Fox M, Rees M, and Lee J-H (1998) Molecular characterization of a neuronal low-voltage activated J-type calcium channel. *Nature (Lond)* **391:**896–899.

Randall A and Tsien RW (1995) Pharmacological dissection of multiple types of Ca^{2+} channel currents in rat cerebellar granule neurons. *J Neurosci* **15:**2995–3012.

Regan LJ (1991) Voltage-dependent calcium currents in Purkinje cells from rat cerebellar vermis. *J Neurosci* **11:**2259–2269.

Scott RH, Dolphin AC, Bindokas VP, and Adams ME (1990) Inhibition of neuronal Ca^{2+} channel currents by the funnel web spider toxin. *Mol Pharmacol* **38:**711–718.

Shapiro MS and Hille B (1993) Substance P and somatostatin inhibit calcium

channels in rat sympathetic neurons via different G protein pathways. *Neuron* **10:**11–20.

Snutch TP, Leonard JP, Gilbert MM, Lester HA, and Davidson N (1990) Rat brain expresses a heterogeneous family of calcium channels. *Proc Natl Acad Sci USA* **87:**3391–3395.

Soong TW, Stea A, Hodson CD, Dubel SJ, Vincent SR, and Snutch TP (1993) Structure and functional expression of a member of the low voltage-activated calcium channel family. *Science (Washington DC)* **260:**1133–1136.

Stapleton A, Blankenship DT, Ackermann BL, Chen TM, Gorder GW, Manley GD, Palfreyman, MG, Coutant JE, and Cardin AD (1990) Curtotoxins: neurotoxic insecticidal polypeptides isolated from the funnel web spider *Holena curta*. *J Biol Chem* **265:**2054–2059.

Stea A, Soong TW, and Snutch TP (1995a) Determinants of PKC-dependent modulation of a family of neuronal calcium channels. *Neuron* **15:**929–940.

Stea A, Soong TW, and Snutch TP (1995b) Voltage-gated calcium channels, in *Handbook of Receptors and Channels: Ligand- and Voltage-Gated Ion Channels* (North RA, ed) pp 113–152, CRC Press, Boca Raton, FL.

Stea A, Tomlinson WJ, Soong TW, Bourinet E, Dubel SJ, Vincent SR, and Snutch TP (1994) The localization and functional properties of a rat brain α1A calcium channel reflect similarities to neuronal Q- and P-type channels. *Proc Natl Acad Sci USA* **91:**10576–10580.

Swartz KJ, Mintz IM, Boland LM, and Bean BP (1993) Block of calcium channels in central and peripheral rat neurons by an ω-conotoxin-MVIIC. *Soc Neurosci Abstr* **19:**607.

Takahashi T and Momiyama A (1993) Different types of calcium channels mediate central synaptic transmission. *Nature (Lond)* **366:**156–158.

Turner TJ, Adams ME, and Dunlap K (1992) Calcium channels coupled to glutamate release identified by ω-Aga IVA. *Science (Washington D C)* **258:**310–313.

Yan LZ, Olivera BM, and Adams ME (1995) Characterization of ω-neurotoxin binding sites on calcium channels. *Soc Neurosci Abstr* **21:**140.8.

Zamponi GW, Bourinet E, Nelson D, Nargeot J, and Snutch TP (1997) Crosstalk between G proteins and protein kinase C is mediated by the calcium channel α1 subunit linker. *Nature (Lond)* **385:**442–446.

Zhang J-F, Randall AD, Ellinor PT, Horne WA, Sather WA, Tanabe T, Schwarz TL, and Tsien RW (1993) Distinctive pharmacology and kinetics of cloned neuronal Ca^{2+} channels and their possible counterparts in mammalian CNS neurons. *Neuropharmacology* **32:**1075–1088.